LA-UR-93- 2068

Title: A Simple Hydrodynamic Model for Jetting from Tubular Hypervelocity Penetrators

Author(s): James R. Kamm, EES-3

Submitted to: Joint AIRAPT/APS Conference on
High Pressure Science and Technology
June 28 - July 2, 1993

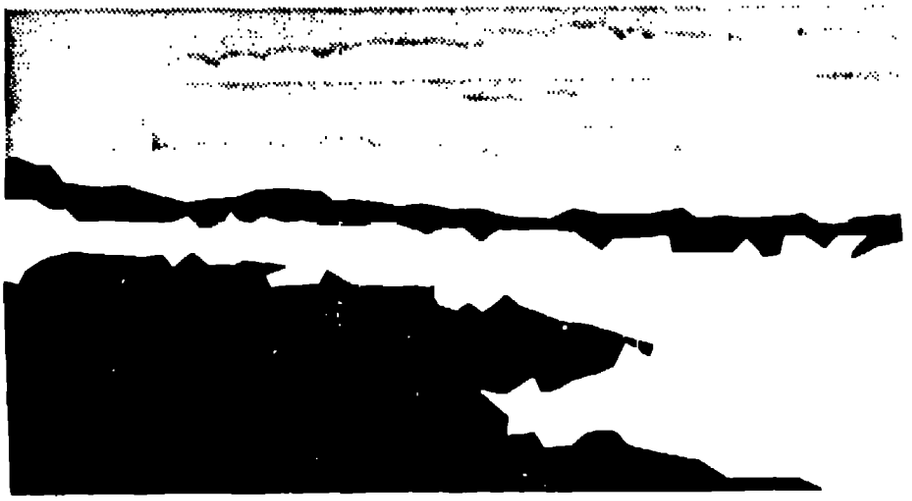

Los Alamos
NATIONAL LABORATORY

A SIMPLE HYDRODYNAMIC MODEL FOR JETTING FROM TUBULAR HYPERVELOCITY PENETRATORS

James R. Kamm
Geophysics Group, MS F659
Los Alamos National Laboratory, Los Alamos, NM 87545 USA

Recent experimental results of Franzen & Schneidewind [1] for the impact of tubular penetrators at 2-4 km/s show the formation of a jet of material ejected from within the interior cavity of the penetrator. Using a simple hydrodynamic model based on the tubular penetration theory of Franzen [2] we calculate steady configurations of outflowing penetrator and target material. From these results, the limiting velocity of the jetting material is obtained and compared with Franzen & Schneidewind's experimental data.

INTRODUCTION

Franzen & Schneidewind [1] (hereinafter F & S) give a brief review of previous work on tubular penetrators. In this work, F & S also present results of reverse ballistic experiments for the normal impact of tungsten, steel, and aluminum tubular penetrators with steel and aluminum targets, including radiographs of experimental impacts that show the presence of a jet of material that is ejected from the hollow interior of the penetrator. The jet, which consists of a high speed precursor element followed by the main body, was not present in all experiments, a fact that F & S attribute to interaction between the jet and the inner wall of the impacting penetrator.

In this work we present a simple hydrodynamic model of tubular rod penetration that is based closely on the formulation developed by Franzen [2], which we modify to allow jetting from within the penetrator cavity. From the assumption of steady, incompressible flow, we obtain values for the velocity of the jet of target material that is ejected during the steady penetration process. We compare these results with the experimentally measured velocities of the precursor jet and the tip of the main jet body.

STEADY HYDRODYNAMIC MODEL

The hydrodynamic model we consider is based upon the assumption that the flow velocities are sufficiently great so that material strength effects can be neglected. With this assumption, the constant penetration velocity U_0 is related to the impact velocity V and the densities of the target ρ_t and penetrator ρ_p as [3]

$$U_0 = \frac{V}{1 + \sqrt{\rho_t/\rho_p}} \tag{1}$$

Assuming that the penetration velocity is less than the sound speed of the target material, we model the steady penetration process as the flow of an inviscid, incompressible fluid. By a uniform translation at the penetration velocity U_0 we obtain a frame of reference in which the bottom of the crater is not moving. The side view of this steady penetration configuration above the axis of symmetry is presented in Fig. 1. We assign the penetrator outer radius to be unity, and denote the inner radius of the penetrator by μ.

Following Franzen [2], the contours of the outflowing penetrator material in Fig. 1 are identified with the subscript i for flow inside the hollow cavity of the incoming penetrator, and the subscript o for flow outside. The widths of the layers of outgoing penetrator material, denoted by τ_i and τ_o, are assumed symmetric about the respective centerline curves, (x_i, y_i) and (x_o, y_o). These quantities are functions of the angle β between the direction tangent to the local centerline of the outflowing penetrator material and the axis of symmetry, where $-\pi/2 \le \beta \le 0$ for flow inside the penetrator, and $0 \le \beta \le \pi/2$ for flow outside.

The fraction of penetrator material that flows inside the penetrator cavity is denoted q, so that the fraction flowing outside is $1 - q$. Mass conservation implies that the inner and outer widths are given by

$$\tau_i(\beta) = \frac{q(1-\mu^2)}{2\,y_i(\beta)}, \quad \tau_o(\beta) = \frac{(1-q)(1-\mu^2)}{2\,y_o(\beta)}. \tag{2}$$

The contours of the outflowing penetrator material inside the cavity can be expressed as

$$\left.\begin{matrix} x_{ri}(\beta) \\ x_{io}(\beta) \end{matrix}\right\} = x_i(\beta) \mp \frac{1}{2}\tau_i(\beta)\sin\beta,$$

$$\left.\begin{matrix} y_{ri}(\beta) \\ y_{io}(\beta) \end{matrix}\right\} = y_i(\beta) \mp \frac{1}{2}\tau_i(\beta)\cos\beta \tag{3}$$

The radius of the target material flowing through the cavity has the value μ at the entrance, and decreases to the value μ^* infinitely far downstream. The mass fraction q of penetrator material flowing inside the cavity is shown by Franzen [2] to be

$$q = \left[2 + \rho_{t,\mathrm{int}}/(\rho_t U_{\mathrm{int}}^2)\right]^{-1}. \tag{4}$$

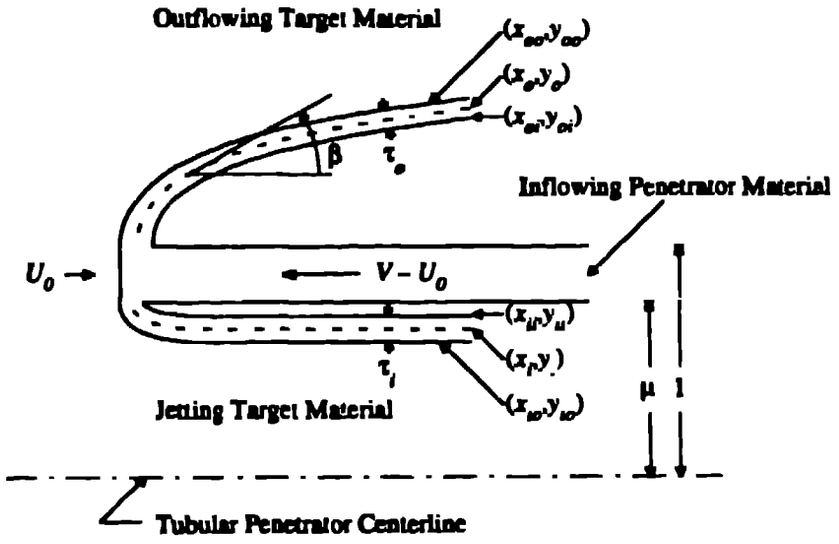

Figure 1. Side view of the impact of a tubular penetrator above the axis of symmetry in the steady frame. The penetrator, which has outer radius unity and inner radius μ, is moving from right to left at velocity $V - U_0$, where V is the impact velocity and U_0 is the hydrodynamic penetration velocity. The finely dashed lines represent the centerlines of the outflowing penetrator material outside (o) and inside (i) the penetrator. The angle between the local centerline tangent and the symmetry axis is denoted β.

where p_s is the static pressure, U is the flow velocity, and *ent* denotes values at the entrance to the cavity.

To determine the inner flow contour, we make the following assumption: in the frame of reference in which the interface between target and penetrator at the bottom of the crater is not moving, *the flow of target material into the cavity occurs at the penetration velocity*, i.e., $U_{ent} = U_0$. This differs from the condition posited by Franzen [2], who requires that the target material flow into the cavity at an undetermined velocity (less than U_0) and reach the velocity U_0 infinitely far downstream; implicit in Franzen's approach is that there is *no* hydrodynamic jetting of target material.

The jet velocity at any downstream position identified by β is related to the local cavity radius and the inflow penetration velocity and radius as

$$U(\beta) = \left(\frac{\mu}{y_o(\beta)}\right)^2 U_0 \quad \rightarrow \quad U^* = \left(\frac{\mu}{\mu^*}\right)^2 U_0, \quad (5)$$

where the limiting value U^* is the velocity infinitely far downstream (i.e., as $\beta \rightarrow 0$). The static pressure p_s of the outflowing target material decreases from its initial value $p_{s,ent}$ to the value zero as $\beta \rightarrow 0$ according to the Bernoulli relation $p_{s,ent} + \frac{1}{2}\rho_t U_0^2 = \frac{1}{2}\rho_t U^{*2}$. Using Eqs. 4 and 5, the following expressions for the pressure at the cavity entrance and for the inward flowing penetrator mass fraction are obtained

$$p_{s,ent} = \frac{1}{2}\rho_t U_0^2 \left[(\mu/\mu^*)^4 - 1\right],$$
$$q = \frac{2}{3 + (\mu/\mu^*)^4} \quad (6)$$

There are two limits for which these expressions are easily examined: (1) the "cookie cutter" limit of a tubular penetrator with a vanishingly thin wall: $\mu \rightarrow 1^-$, and (2) the solid rod limit: $\mu \rightarrow 0^+$. In the first case, assuming that the jet radius also approaches unity implies that the jet velocity reduces to the penetration velocity (i.e., there is no jetting in the laboratory frame of a zero velocity target), the static pressure at the cavity entrance goes to zero, and half of the penetrator material flows inside the cavity. In the solid rod case, assuming that the jet radius vanishes faster than the cavity inflow radius (i.e., $\mu^* = o(\mu)$ as $\mu \rightarrow 0^+$) implies that both the jet velocity and the static pressure at the cavity entrance grow without bound, and all penetrator material flows outside of the cavity; these limiting values for the jet velocity and cavity entrance pressure are clearly unphysical, indicating that our model is inappropriate in the solid rod limit.

Following Franzen [2], we assume that the internal flow is governed by the balance between the normal force due to the dynamic and static pressure in the outflowing target material and the normal force due to the centripetal acceleration of the outflowing penetrator material. This balance is expressed in the equation

$$\frac{1}{2}\rho_t U^2(\beta)\sin^2\beta + p_s(\beta) - r_i(\beta)\rho_p \frac{(V - U_0)^2}{R(\beta)}, \quad (7)$$

where $R(\beta) = \csc\beta\,(dy_i/d\beta)$ is the radius of curvature of the of the inner centerline curve. Using Eqs. 1, 2, 3, 5, and the Bernoulli relation, this equation simplifies to the following first order ODE for the centerline y coordinate of the interior flow contour

$$\frac{dy_i}{d\beta} = \frac{1}{y_i}\left[(1-\mu^2)\,q\,\sin\beta\right] \cdot \left\{\left(\frac{\mu}{\mu^*}\right)^4 - \frac{\mu^4 y_i^4 \cos^2\beta}{\left[y_i^2 - \frac{1}{4}(1-\mu^2)\,q\cos\beta\right]^4}\right\}^{-1} \quad (8)$$

This equation is subject to two boundary conditions, viz., (1) at inflow, the centerline value is the inner radius of the penetrator; and (2) at outflow, the inner contour height is the jet radius. These boundary conditions are expressed mathematically as:

$$y_i(-\pi/2) = \mu\,,$$
$$y_i(0) = \frac{\mu^*}{2}\left\{1 + \sqrt{1 + [q(1-\mu^2)]/\mu^{*2}}\right\}. \quad (9)$$

Eqs. 8 and 9 constitute a two-point boundary value problem for y_i with the eigenvalue μ^*. The axial coordinates of the associated flow contours are related to the radial coordinates through the geometric relation $dy_i/dx_i = \tan\beta$.

Substitution of the following variables:

$$w \equiv y_i^2, \quad \lambda \equiv \mu^2, \quad \lambda^* \equiv \mu^{*2}, \quad \xi \equiv \cos\beta, \quad (10)$$

simplifies Eqs. 8, 9 to the following form:

$$\frac{dw}{d\xi} = -2(1-\lambda)q \cdot \left\{\left(\frac{\lambda}{\lambda^*}\right)^2 - \left(\frac{\lambda w \xi}{\left[w - \frac{1}{4}(1-\lambda)\,q\,\xi\right]^2}\right)^2\right\}^{-1},$$
$$w(\xi = 0) = \lambda\,,$$
$$w(\xi = 1) = \frac{\lambda^*}{4}\left\{1 + \sqrt{1 + [q(1-\lambda)]/\lambda^*}\right\}^2. \quad (11)$$

These equations can be analyzed in the "cookie cutter" limit $\lambda \to 1$. Assuming that λ^* decreases from the limiting value of unity faster than λ, we employ the following expansions (where $0 < \epsilon \ll 1$):

$$w = 1 - \epsilon v + o(\epsilon), \quad \lambda = 1 - \epsilon + o(\epsilon) \quad (12)$$

Substituting these quantities into Eq. 11 and imposing the boundary condition at $\xi = 0$ yields the following solution for the leading order term:

$$v = \frac{2\lambda^{*3}}{1 + 3\lambda^{*2}} \log\left(\frac{1 + \lambda^*\xi}{1 - \lambda^*\xi}\right) \quad (13)$$

Analysis of the boundary condition $v = 1$ implies that the expansion for λ^* should be of the form:

$$\lambda^* = 1 + \ell_1 \epsilon \log\epsilon + \ell_2 \epsilon \log|\log\epsilon| + \ell_3 \epsilon + o(\epsilon) \quad (14)$$

Substituting this expression into the boundary condition given in Eq. 11, equating like terms, and solving the resulting equations yields the following values for the perturbation coefficients:

$$\ell_1 = \frac{1}{2}\,,\ \ell_2 = \frac{1}{2}\,,\ \ell_3 = -\left(\frac{5}{4} + \log 2\right) \approx -1.94\,. \quad (15)$$

RESULTS

An initial solution to Eqs. 8 and 9 was found using the relaxation method [4] for a value of μ near unity with an initial guess for μ^*; other members of the family of solutions parameterized by μ were obtained by continuation in μ away from the initial converged solution. The results for the limiting nondimensional jet radius as a function of the ratio of penetrator inner radius to outer radius are given in Figure 2. When μ approaches the limiting "cookie cutter" value of unity, the jet radius also approaches unity; as the thickness of the penetrator wall is increased, the jet radius decreases. Numerical solutions were obtained down to the value of $\mu = 0.1$; below this value, the computed limiting jet velocity is almost an order of magnitude greater than the penetration velocity, a situation we suspect to be physically unlikely. Plotted as a dashed line in Fig. 2 is the value of μ^* computed by Franzen [2] under the assumption that there is no hydrodynamic jetting. Whereas our model gives a nonzero limiting jet radius for tubular penetrators of all thickness ratios chosen, the zero-jet assumption implies that the center cavity converges on axis for $\mu \lesssim 0.69$, for which no flow configuration solution was obtained. The dotted line in the inset to Fig. 2 is the perturbation solution, through and including the $O(\epsilon)$ term, for $0 < \epsilon \leq 0.1$.

Figure 3 depicts the results for the computed jet velocity normalized by the hydrodynamic penetration velocity in the laboratory frame (i.e., the frame in which the penetrator has speed V and the target is stationary) as a function of the ratio of penetrator inner radius to outer radius. There is no jetting in the "cookie cutter" limit, and the limiting jet velocity increases as the nondimensional inner radius of the penetrator decreases. The dotted line in the inset to Fig. 3 is the perturbation solution, through and including the $O(\epsilon)$ term, for $0 < \epsilon < 0.1$. Also shown on this diagram are the experimental values presented by F & S for the precursor velocity (denoted with a circle) and the velocity of the tip of the main jet (denoted with a cross), normalized by the hydrodynamic penetration velocity computed according to Eq. 1 for the materials involved, assuming the following mass densities: $\rho_W = 19.2$ g/cc, $\rho_{steel} = 7.8$ g/cc, and $\rho_{Al} = 2.7$ g/cc. The numerical values of the experimental data and the corresponding model results are presented in Table 1. The limiting jet velocity predicted by the hydrodynamic model compares moderately well with the experimental data for the precursor jet, which may consist of ejected target material liberated by high tensile stresses. This favorable

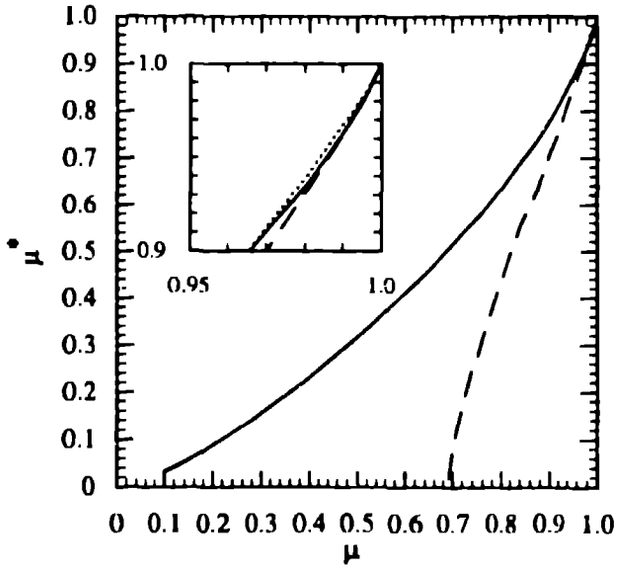

Figure 2. Computed limiting nondimensionalized jet radius as a function of the ratio of inner radius to outer radius of the tubular penetrator. The solid line represents the results of the present investigation, the dashed line denotes the non-jetting limiting cavity radius values according to Franzen [2], and the dotted line in the inset is the perturbation solution, through and including the $O(\varepsilon)$ term.

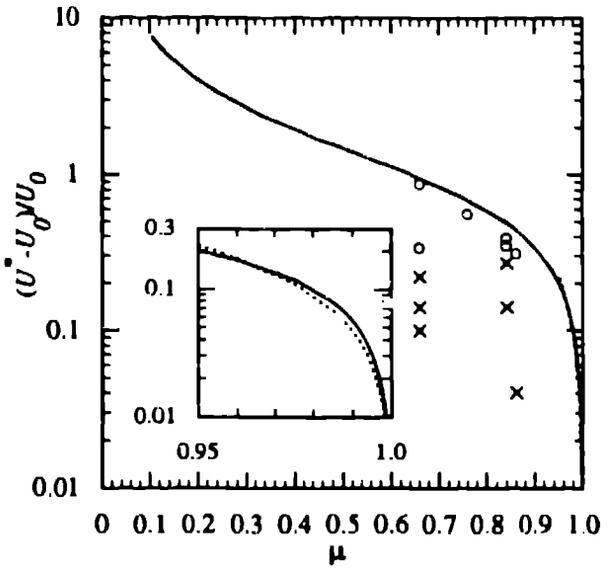

Figure 3. Computed limiting nondimensionalized lab frame jet velocity versus the ratio of inner to outer radius of the tubular penetrator. The dotted line in the inset is the perturbation solution, through and including the $O(\varepsilon)$ term. Experimental data of F & S [1] for impacts of W, steel, and Al penetrators on steel and Al targets are depicted as o for precursor jet velocity, and x for main jet velocity.

Table 1. Experimental and computed jet velocities for the impact of tubular penetrators.

F & S Test #	Pen. Material	Target Material	μ	V (km/s)	U_0 (km/s)	Experimental U_{tip}/U_0	Experimental U_{prec}/U_0	Comp. U_{jet}/U_0
HT-15	W	Steel	0.84	2.17	1.33	0.26	0.35	0.49
HT-16	W	Steel	0.84	2.26	1.38	0.14	0.39	0.49
HT-17	W	Steel	0.66	2.04	1.25	0.22	0.88	0.95
HT-18	W	Steel	0.66	2.04	1.25	0.14	-	0.95
HT-24	Steel	Al	0.86	3.59	2.26	0.04	0.31	0.44
HT-25	Steel	Al	0.76	3.63	2.29	-	0.56	0.69
HT-27	Al	Al	0.66	4.00	2.00	0.10	0.34	0.95

comparison is interesting, as we have neglected the effects of compressibility and material strength, both of which play significant roles in the phenomenology of cratering and ejecta formation. The "ballpark" agreement between the computed jet velocities and experimental precursor velocities suggests that basic hydrodynamics may provide a useful model for the jetting of material during the quasi steady phase of penetration following the impact of tubular rods at moderately high velocities.

ACKNOWLEDGEMENTS

This work was begun when the author was at SAIC. The author thanks R. Stoughton for his support of this investigation, J. Rotenberry for helpful insights into the perturbation analysis, K. McCall for valuable suggestions on the text, and M. Scharff for the introduction to hypervelocity impact phenomenology.

REFERENCES

1. R. R. Franzen and P. N. Schneidewind, Observations Concerning the Penetration Mechanics of Tubular Hypervelocity Penetrators, *Int. J. Impact. Engng* 11, No. 3, pp. 289-303 (1991).
2. R. R. Franzen, "Notes on Tubular Hypervelocity Penetrators," in *Proceedings of the 10th International Symposium on Ballistics*, San Diego, CA 1987.
3. G. Birkhoff, D. P. MacDougall, E. M. Pugh and G. I. Taylor, Explosives with Lined Cavities, *J. Appl. Physics* 19, pp. 563-582 (1948).
4. W. H. Press, B. P. Flannery, S. A. Teukolsky and W. T. Vetterling, *Numerical Recipes, The Art of Scientific Computing*, Cambridge University Press, 1986.